CERN – EUROPEAN ORGANIZATION FOR NUCLEAR RESEARCH

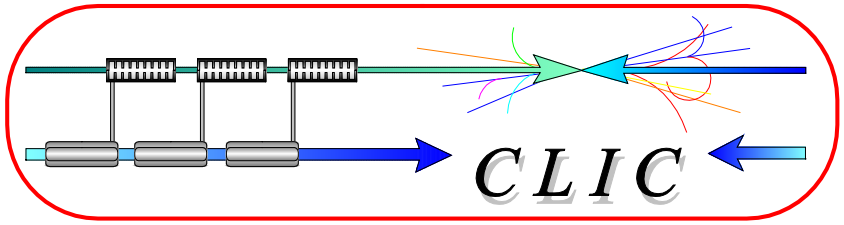

CLIC – Note - 819

THE CLIC POSITRON CAPTURE AND ACCELERATION IN THE INJECTOR LINAC

A. Vivoli[1], I. Chaikovska[2], R. Chehab[3], O. Dadoun[2], P. Lepercq[2], F. Poirier[2], L. Rinolfi[1], V. Strakhovenko[4], A. Variola[2]

[1] CERN, 1211 Genève, Switzerland
[2] LAL, IN2P3-CNRS and Université de Paris-Sud, 91898, Orsay, France
[3] IPN-Lyon, IN2P3-CNRS and Université Claude Bernard, 69622, Villeurbanne, France
[4] BINP, 630090 Novosibirsk, Russia

Abstract

The baseline of the CLIC study considers non-polarized e^+ for the 3 TeV centre of mass energy. The e^+ source is based on the hybrid targets scheme, where a crystal-radiator target is followed by an amorphous-converter target. Simulations have been performed from the exit of the amorphous target up to the entrance of the Pre-Damping Ring. Downstream the amorphous target, there is an Adiabatic Matching Device (AMD) followed by a Pre-Injector Linac accelerating the e^+ beam up to around 200 MeV. Then a common Injector Linac (for both e^+ and e^-) accelerates the beams up to 2.86 GeV before being injected into the Pre-Damping Ring. In this note, the characteristics of the AMD and the other sections are described and the beam parameters at the entrance of the Pre-Damping Ring are given.

Geneva, Switzerland
15 June 2010

1. Introduction

The Compact Linear Collider (CLIC) 3 TeV (center of mass energy) design requires $3.72 \cdot 10^9$ particles per bunch, 312 bunches per train (0.5 ns bunch spacing) and 1 train per pulse at a repetition rate of 50 Hz for the e^- and e^+ beams at the interaction point [1]. A configuration at 500GeV with basically double charge per bunch is also foreseen [2]. To generate and transport these beams, a Main Beam Injector Complex has been designed [3] including the e^- and e^+ sources.

Focusing on the e^+ source and the issues related to it, it should be pointed out that the main constraint for the production of the e^+ beam comes from target survivability requirement. In e^+ sources positrons are created by photons, undergoing pair production, interacting with nuclei in an amorphous target. In the CLIC positron source design this is realized by the hybrid target scheme [4], which consists in sending a 5 GeV e^- beam into a thin crystal target (in Tungsten) where electrons emit channeling radiation toward an amorphous thick target (also in Tungsten), while charged particles coming out of the crystal are swept out by a dipole magnet placed between the two targets, separated by a distance of 2 m; such system was proposed for CLIC by R. Chehab, V. Strakhovenko and A. Variola. Different processes take place in the targets, caused by the impinging particles, and a certain amount of energy is deposited in there. One source of damage for the targets comes from the average power deposited, that causes the target heating, while another one comes from the Peak Energy Deposition Density (PEDD) that can cause target breakdown. While the first problem can be solved (for the CLIC positron source) using an efficient target cooling system to prevent the target to be exposed to excessive heating, the second problem can only be avoided by limiting the maximum energy density deposited in each time interval of some μs [5]. This last constraint clearly sets a limit to the total charge of the primary e^- beam impinging the crystal and demands that a sufficiently high yield (defined as the ratio between the number of e^+ delivered at a given point and the number of electrons in the primary e^- beam) is reached in the positron source.

In this note the CLIC positron source is described according to the baseline design, including the targets, the Adiabatic Matching Device (AMD), the Pre-Injector Linac, bunch compressor and Injector Linac up to the injection in the CLIC Pre-Damping Ring. For each element the results of simulations are given.

2. Layout of the e^+ source

The CLIC positron source (see layout in Figure 1) is composed of an electron gun, generating the primary e^- beam, followed by a bunching system and a 2 GHz linac, accelerating the beam up to 5GeV and a bunch compressor to reach a bunch length of 1ps (0.3 mm). The primary e^- beam is sent to a tungsten crystal target oriented along its <111> axis.

The channeled electrons of the primary e^- beam emit radiation toward an amorphous tungsten target placed downstream the crystal. A dipole magnet is also inserted between the two targets to sweep away the charged particles exiting the crystal.

Positrons and electrons are created by pair production from the gammas impinging the amorphous target followed immediately by the AMD chosen as matching device to capture the charged particles.

At the end of the AMD a 2 GHz Pre-Injector Linac accelerates the particles up to about 200MeV. The whole Pre-Injector Linac is inserted inside a solenoid where the axial magnetic field is used to prevent the beam envelope to increase, causing losses in the positron beam. At the end of the Pre-Injector a bunch compressor is placed to reduce the bunch length of the e^+ beam to make it suitable for further acceleration in the Injector Linac and subsequent injection in the Pre-Damping Ring (PDR). The bunch compressor is also used as an energy collimator for the positrons, and also as a device to separate the positrons from the electrons accelerated by the RF field of the Pre-Injector Linac that can be dumped at this place. Finally the e^+ beam is accelerated to the energy of 2.86 GeV by the 2 GHz Injector Linac, and injected in the PDR.

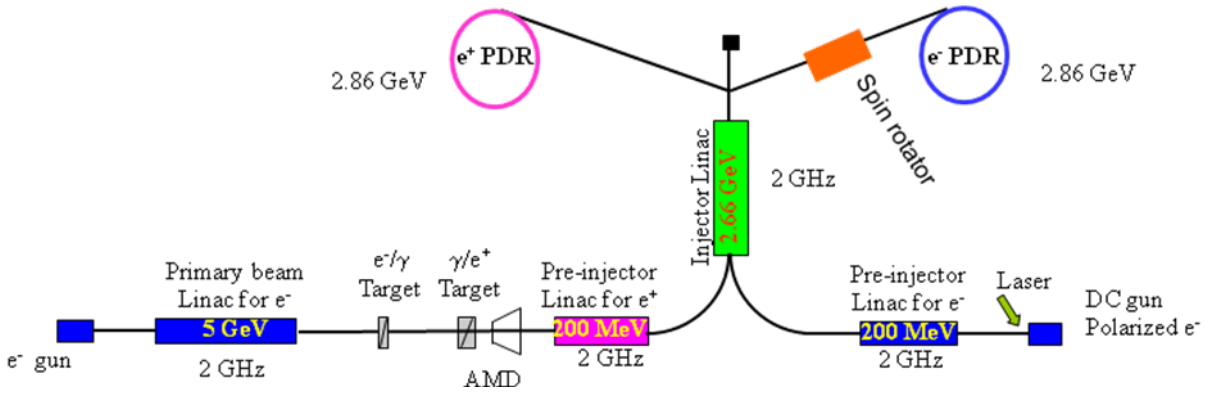

Figure 1 – Layout of the CLIC positron and electron sources.

3. Generation of positrons

3.1 Targets

As already mentioned, positron generation is achieved employing a hybrid target scheme. A detailed study of different choices of targets and parameters available for this scheme, including an evaluation of the PEDD and survivability of the targets, is presented in [6]. The parameters of the e^- beam required at the crystal target are summarized in Table 1.

Table 1 – Primary beam parameters at the crystal target.

Beam Parameter	Unit	Value
N. Bunches/Train		312
Bunch separation	ns	0.5
N. train/pulse		1
Pulse duration	ns	156
Repetition rate	Hz	50
Energy	GeV	5
Bunch Charge	nC	1.63
Bunch length (rms)	ps	1
Bunch radius (rms)	mm	2.5

The thicknesses of the two targets are 1.4mm for the crystal and 10mm for the amorphous. The distance between the 2 targets is 2m. A scheme of the two targets system is shown in Figure 2.

Simulations of the positron production by this scheme have been performed with different codes and the results have been published in [6]. The results of those simulations have been used as input data for the simulations published here. The parameters of the positrons at the exit of the target are presented in Table 2.

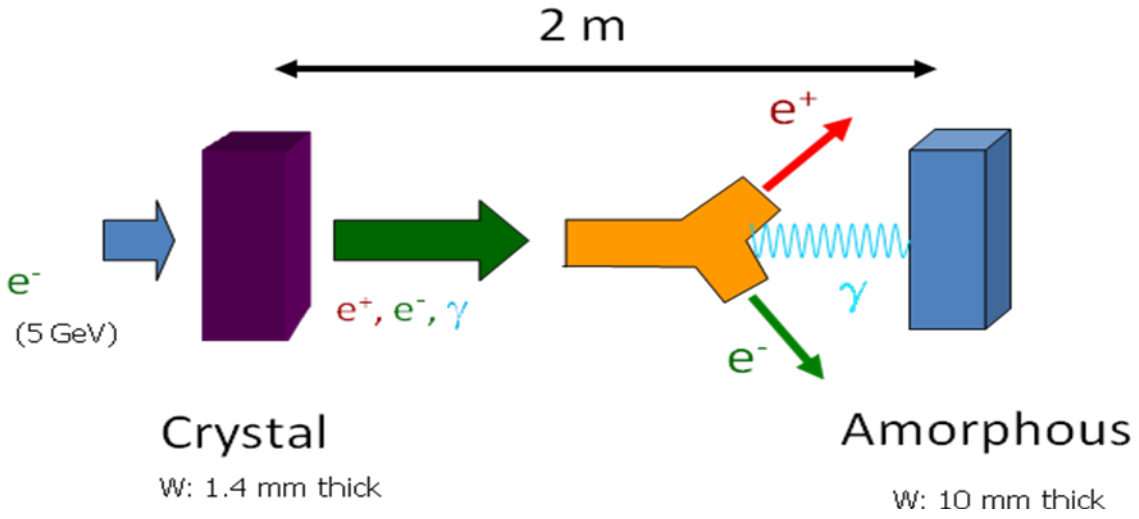

Figure 2 - Layout of the hybrid target scheme.

Table 2 – Positron parameters after the amorphous target.

Beam Parameter	**Unit**	**Value at the target exit**
Yield	e^+/e^-	7.74
Mean energy	MeV	52.6
Horizontal normalized emittance (rms)	m rad	6.50
Vertical normalized emittance (rms)	m rad	4.99
Bunch length (rms)	mm	0.3
Energy spread (rms)	MeV	110

3.2 Adiabatic Matching Device (AMD)

After the amorphous target the AMD is implemented (see Figure 3). In the simulation performed, the magnetic field of the AMD is placed immediately after the amorphous target, but in practice it will be difficult to isolate the target from this field that will surround it. The AMD is used as optical device to match the positron beam at the target exit (with huge transversal divergence and energy spread) to the acceptance of the Pre-Injector Linac. More details about AMD optics can be found in [7]. The advantage of using an AMD as a matching device is that it allows increasing the accepted yield of positrons, capturing particles within a large energy range. Its biggest drawback is a lengthening of the bunch, which is responsible of an increase of the energy spread induced by the curvature of the RF accelerating field in the Pre-Injector Linac. The parameters used for the simulations of the AMD are showed in Table 3. The accepted yield at the exit of the AMD is about 2.1 e^+/e^-. The simulations have been performed using the tracking code ASTRA [8].

Table 3 - AMD Parameters.

Parameter	Unit	Value
Initial axial magnetic field	T	6
Final axial magnetic field	T	0.5
Length	mm	200
Vacuum chamber radius	mm	20

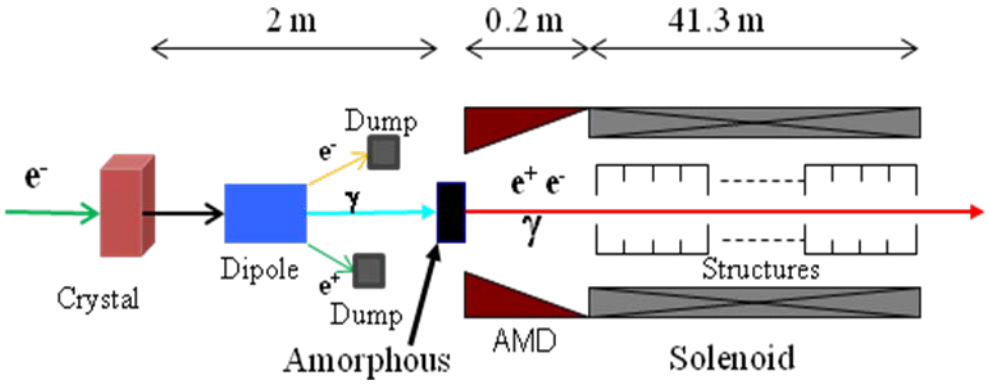

Figure 3 – Layout of the hybrid target scheme, AMD and Pre-Injector Linac.

3.3 Pre-Injector Linac (Pre-Accelerator)

At the end of the AMD (20 cm downstream the amorphous target) it is installed the first accelerating structure of the Pre-Injector Linac, that accelerates the e^+ beam up to the energy of about 200 MeV. The RF frequency is 2 GHz, in order to have the same bunch spacing and beam structure of the interaction point. The present simulations are based on the design of a 2 GHz standing wave accelerating structure, suitable for continuous wave operation mode at a peak accelerating field on the axis equal to 5.2MV/m. However the Pre-Injector Linac will operate in pulsed mode at 50 Hz (see Table 1), therefore the peak accelerating field can be increased to 25 MV/m, which should still be conservative. The parameters of the structure are presented in Table 4. The field in the structure has been calculated with code Poisson Superfish [9] and then used as input field for ASTRA.

Table 4 – Parameters of accelerating structures in Pre-Injector Linac.

Parameter	**Unit**	**Value**
Length	cm	58.97
Frequency	GHz	1.9992
N. cells		6
Phase advance per cell	π	2/3
Axial Electric Field	MV/m	10
Max. Energy Gain	MeV	6

The layout of 2 consecutive accelerating structures of the Pre-Injector Linac is presented in Figure 4. Starting from the end of the AMD it is composed of sequences of 3 consecutive accelerating structures (forming 1.80m accelerating structures) separated by drift of 15cm to leave some space for devices and eventual instrumentation. Strong effort should be made in having a compact acceleration group at the beginning of the linac, since positrons have high transversal momentum and must be accelerated in a short distance to avoid losses and a reduced accepted yield.

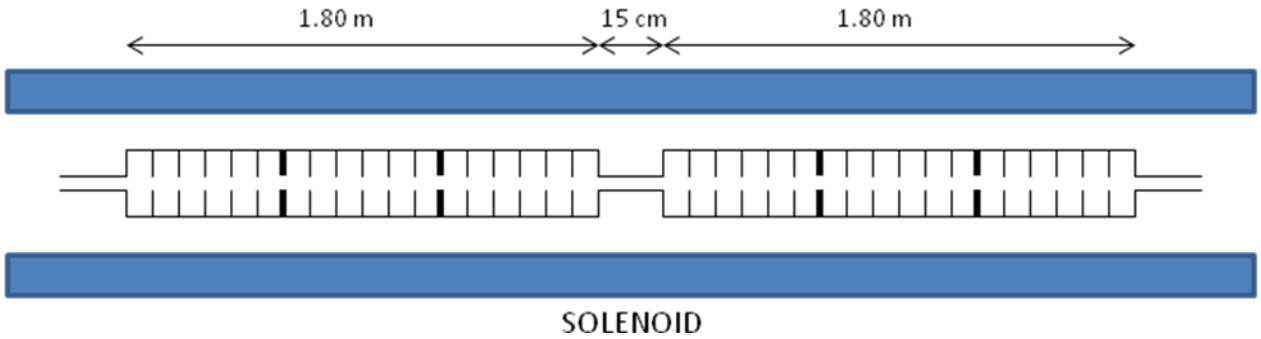

Figure 4 – Two accelerating structures in the Pre-Injector Linac.

The whole Pre-Injector Linac is located inside a solenoid of length 41.30m, and axial magnetic field equal to 0.5T, in order to focus the positrons and avoid losses until their divergence is sufficiently reduced (at 200MeV). The parameters of the Pre-Injector Linac are summarized in Table 5. A peak accelerating field of 25MV/m produces an average accelerating field of 10MV/m for a synchronous particle in the structures, but since the bunch length is not negligible the resulting average accelerating field is 5MV/m. This value multiplied by the structure length gives an acceleration of 8.85MeV. Since there are 21 of such structures in the Pre-Injector Linac the total acceleration is equal to about 186 MeV.

Table 5 – Parameters of the Pre-Injector Linac.

Pre-Injector Linac parameters	**Unit**	**Value**
Total Length	m	41
Frequency	GHz	1.9992
Average Accelerating Field	MV/m	5
Max. Axial Electric Field	MV/m	25
N. accelerating structures		3 X 21
Solenoid length	m	41.3
Axial magnetic field	T	0.5

Table 6 – Beam parameters at the exit of the Pre-Injector Linac.

Beam Parameters	**Unit**	**Value**
Mean energy	MeV	222
Yield	e^+/e^-	0.82
Horizontal Normalized Emittance (rms)	mm mrad	8980
Vertical Normalized Emittance (rms)	mm mrad	8836
Energy spread (rms)	%	23
Bunch length	mm	12.2

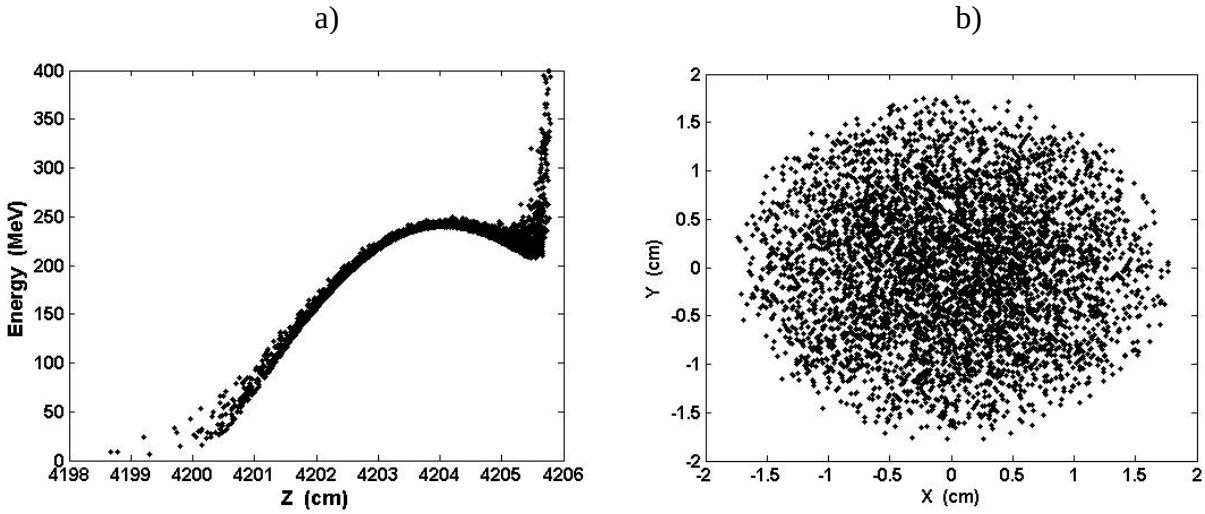

Figure 5 – a) Longitudinal phase space of the beam at the exit of the Pre-Injector Linac. Horizontal axis is the distance downstream the amorphous target. b) Transverse beam size at the same location (42.05m).

The value of the average accelerating field is also due to the fact that the beam is not accelerated 'on crest' in the Pre-Injector Linac in order to maximize the yield of positrons in the final energy range and increase the accepted yield in the Pre-Damping Ring.

The beam parameters at the exit of the solenoid are given in Table 6. Figure 5 shows pictures of the beam phase space resulting from simulations. As it can be seen the bunch length is not small compared to the wavelength of the RF field, resulting in an accentuate curvature of the beam in the longitudinal phase space.

3.4 Bunch Compressor

Following the studies in [10], a bunch compressor is placed at the exit of the solenoid containing the Pre-Injector Linac, with the purpose of reducing the beam energy spread produced by the RF field of the Injector Linac. A layout of the bunch compressor is presented in Figure 6. Before the compression of the beam it is necessary to introduce a longitudinally correlated energy spread which is created by a travelling wave structure having length equal to 3m, placed 5.90m downstream the solenoid. Quadrupoles Q1-6 are used to match the beam to the aperture of the structure. Other 5 quadrupoles (Q7-11) are used as FODO lattice in order to keep the beam focused inside the accelerating structure. Quadrupoles Q8-10 have to wrap the structure and then they need to have bigger aperture (see Table 9). The last 4 quadrupoles (Q12-15) are used to match the beam to the optics of the magnetic chicane, composed of 4 rectangular bending magnets (B1-4), which provides the longitudinal compression of the beam.

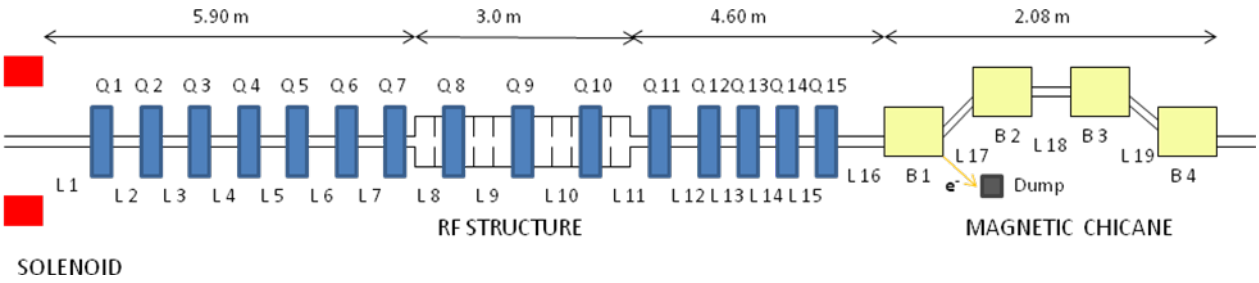

Figure 6 – Layout of the bunch compressor.

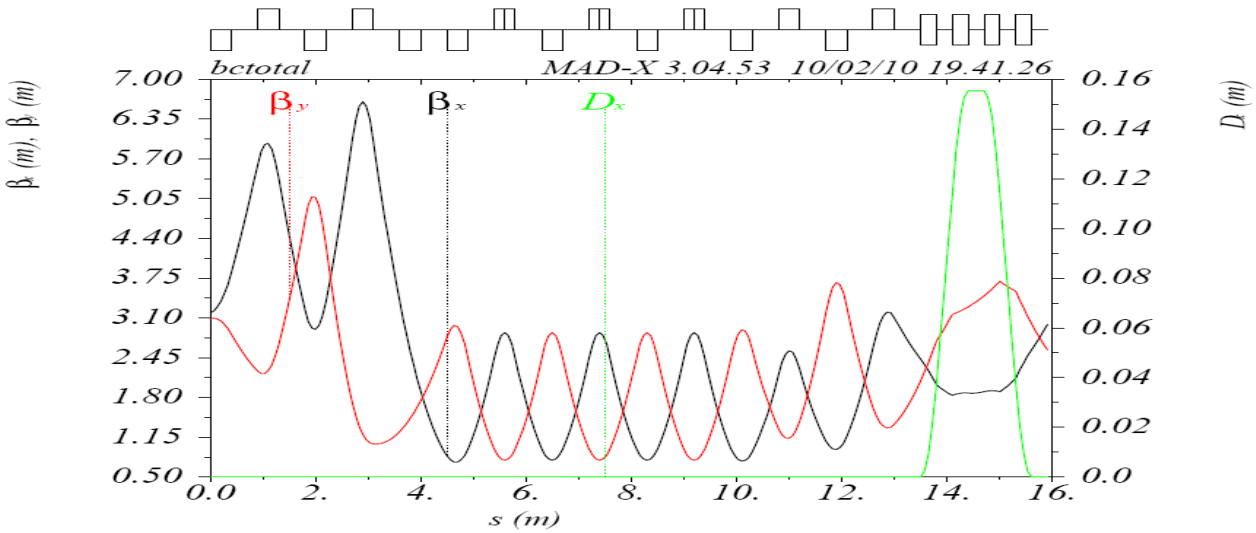

Figure 7 – Optics of the bunch compressor.

The study of the optics of the bunch compressor has been performed with MAD-X [11] and the resulting Twiss functions are presented in Figure 7. The apertures of the elements up to the magnetic chicane are at least 4.3 times the rms transversal beam size assuring a transmission efficiency of the 99.9% of the particles. The parameters of the RF structure used are presented in Table 7. The magnetic chicane composed of 4 rectangular bending magnets (parameters in Table 8) provides a compression factor R_{56}= 66.4mm. The parameters of the quadrupoles used are given in Table 9 while the drift spaces between the elements are reported in Table 10.

Table 7 – Parameters of the RF structure in the bunch compressor.

Parameter	Unit	Value
Length	m	3
Aperture radius	cm	3
Electric Field	MV/m	14.5
Frequency	GHz	1.9992
N. Cells		57
Phase advance per cell	π	2/3

Table 8 – Parameters of the bending magnets in the bunch compressor.

Element	Length (cm)	Magnetic Field (T)	Bending Radius (m)
B1	30	0.5844	1.1773
B 2	30	-0.5844	-1.1773
B 3	30	-0.5844	-1.1773
B 4	30	0.5844	1.1773

Table 9 - Parameters of the quadrupoles in the bunch compressor.

Element	Length (cm)	Gradient (T/m)	Inscribed radius (cm)
Q 1	40	-0.6167	5
Q 2	40	1.4397	5
Q 3	40	-2.1859	5
Q 4	40	1.7844	5
Q 5	40	-0.0309	5
Q 6	40	-2.2537	5
Q 7	40	2.8621	5
Q 8	40	-2.8621	20
Q 9	40	2.8621	20
Q 10	40	-2.8621	20
Q 11	40	2.8621	5
Q 12	40	-2.5792	5
Q 13	40	2.6402	5
Q 14	40	-2.3333	5
Q 15	40	1.7478	5

Table 10 – Parameters of the drift spaces in the bunch compressor.

Element	Length (cm)	Aperture radius (cm)
L1	50	5
L 2	90	5
L 3	90	5
L 4	90	5
L 5	90	5
L 6	90	5
L 7	90	5
L 8	90	3
L 9	90	3
L 10	90	3
L 11	90	3
L 12	90	5
L 13	90	5
L 14	90	5
L 15	90	5
L 16	50	5
L 17	30	5
L 18	30	5
L 19	30	5

The transformations of the bunch in the longitudinal phase space are showed in Figure 8. As it can be seen from the picture, the bunch compressor does not perform an optimal compression of the bunch. This is intentionally done in order to not increase the energy spread of the beam before the injector linac, which would produce an emittance growth due to chromatic effects. It is more convenient to use the bunch compressor to concentrate most of the particles in a short region at the head of the beam such that they receive uniform acceleration and can be injected inside the acceptance area of the PDR.

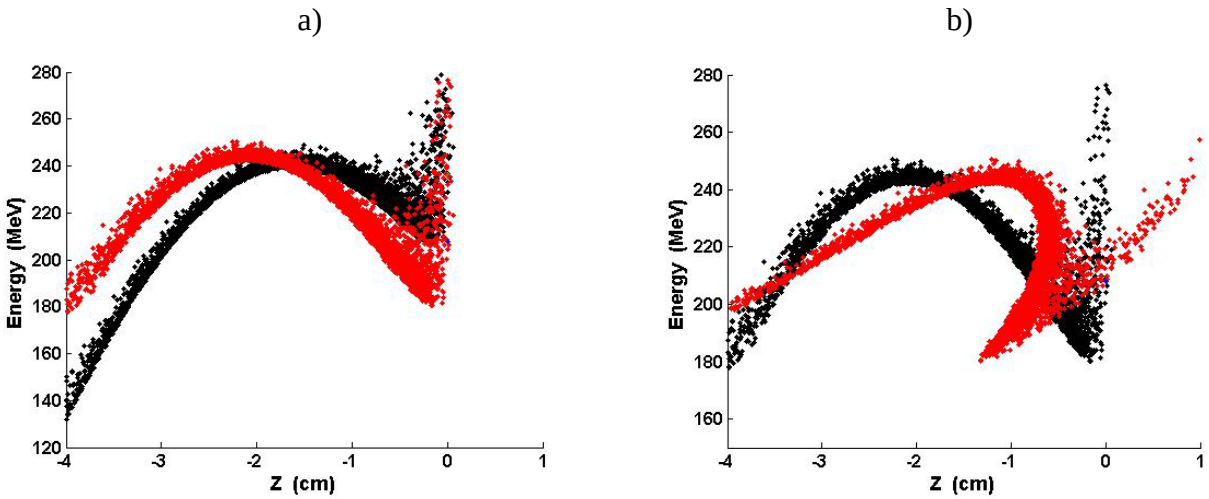

Figure 8 – a) Longitudinal phase space of the positron bunch before (black) and after (red) the RF structure. b) Longitudinal phase space before and after the magnetic chicane (same convention for the colors).

As can be seen in Figure 7, in straight section L18 the dispersion is maximal. Figure 9 shows the horizontal displacement of the particles from the axis of elements B1 – B4. Particles with higher energy have a horizontal displacement reduced compared to lower energy particles and it is possible to perform an energy collimation inserting a horizontal diaphragm at this point. In this way one can get rid of particles with energy too high or too low which would be lost in the Injector Linac due to their different focusing or not successfully injected in the PDR because of the limited energy acceptance. In the simulations it is assumed a horizontal diaphragm of radius 3.6cm, centered at position X = -15.4cm.

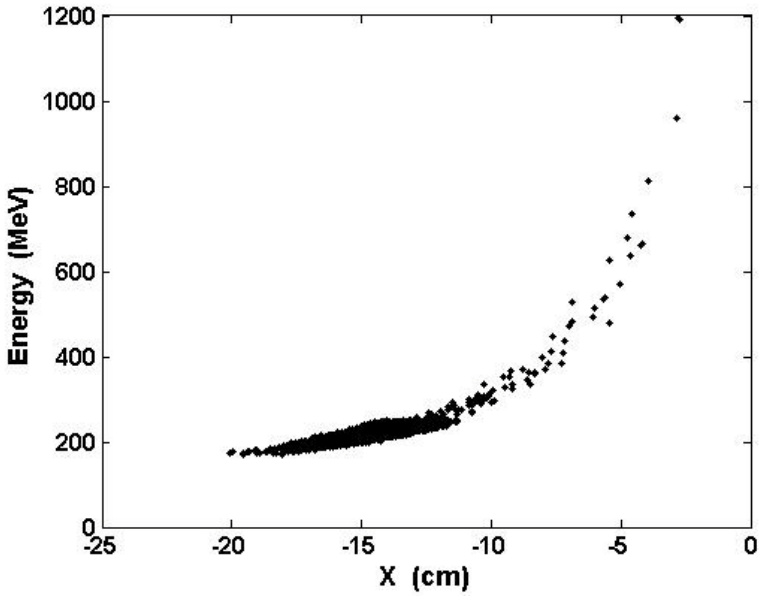

Figure 9 – Horizontal displacement of the particles from the axis of the elements B1-B4. A diaphragm is placed from position x= -19.0 cm to x= -11.8 cm.

The bunch parameters of the e^+ beam at the end of the bunch compressor are listed in Table 11. The bunch compressor at this point can also be useful to dump electrons coming out of the amorphous target and accelerated up to the end of the Pre-Injector Linac in the negative phase buckets of the RF field. Since they are bent in the opposite direction compared to the positrons, a dump can be placed after bending magnet B1 to dispose of them (see Figure 6).

Table 11 – Parameters of the positron beam at the end of the bunch compressor.

Beam Parameters	**Unit**	**Value**
Mean energy	MeV	220
Yield	e^+/e^-	0.754
Horizontal Normalized Emittance (rms)	mm mrad	7810
Vertical Normalized Emittance (rms)	mm mrad	7668
Energy spread (rms)	%	8
Bunch length (rms)	mm	9.2

Simulations of the magnetic chicane have been performed with the software CSRtrack [12].

3.5 Injector Linac

After the bunch compressor, the Injector Linac accelerates the particles up to 2.86GeV (injection energy of the PDR). This linac is common to positrons and electrons, but since the emittance of the e^+ beam is much bigger than the emittance of the e^- beam, only the simulation of the former one will be discussed.

The acceleration of the particles is provided by a total number of 47 travelling wave accelerating structures 3.90 m long, working at the frequency of 2 GHz. The loaded gradient is 14.6 MV/m providing an energy gain of 56.95MeV per structure. The parameters of the accelerating structures are summarized in Table 12.

Table 12 – Parameters of the accelerating structures in the Injector Linac.

Parameter	**Unit**	**Value**
Length	m	3.9
Aperture radius	mm	30
Electric Field	MV/m	14.6
Frequency	GHz	1.9992
Energy gain	MeV	56.95
N. Cells		75
Phase advance per cell	π	2/3

Concerning the optics, the present design follows basically the one presented in [10], with the difference that the Injector Linac is divided in 3 sections.

3.5.1 First section of Injector Linac

The first section is composed of the first 11 structures, separated by a distance of 1.50m. The focusing of the beam is provided by a FODO lattice which alternates focusing quadrupoles of type ‘Qf1’ and defocusing ones of type ‘Qd1’, separated by a distance of 50cm. A quadrupole Qd1 followed by a quadrupole Qf1 forms a FODO cell. Each FODO cell is separated from the next one by 50cm. Each accelerating structure is then covered by 3 FODO cells for a total of 66 cells in the FODO section of the Injector Linac. The length of each quadrupole is 40cm. The radius aperture is 5cm for quadrupoles between accelerating structures and 20 cm for quadrupoles wrapping the accelerating structures.

The layout of the FODO section of the injector linac for the first 2 accelerating structures (‘ACS1’ and ‘ACS2’) is illustrated in Figure 10 together with the matching section composed of 6 quadrupoles (Q16-21) which is used to match the beam coming out of the magnetic chicane of the bunch compressor to the optics of the FODO lattice. The parameters of the matching system and FODO cells are reported in Tables 13 and 14. The design of the optics in the Injector Linac has been studied using MAD-X and the result for the calculation of the Twiss functions in the FODO section is presented in Figure 11.

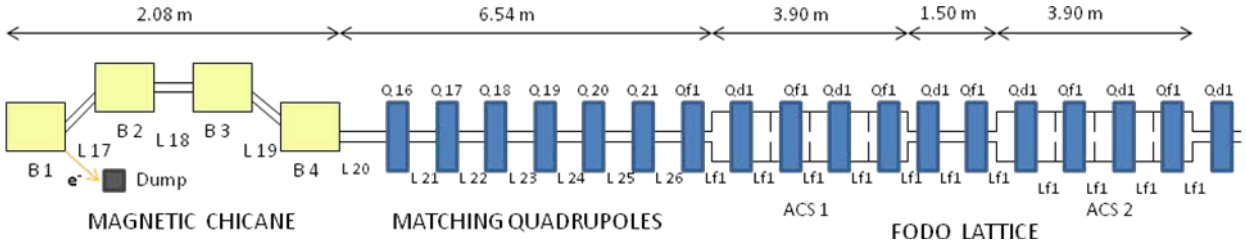

Figure 10 – Matching system and FODO lattice of the Injector Linac (for the first 2 structures).

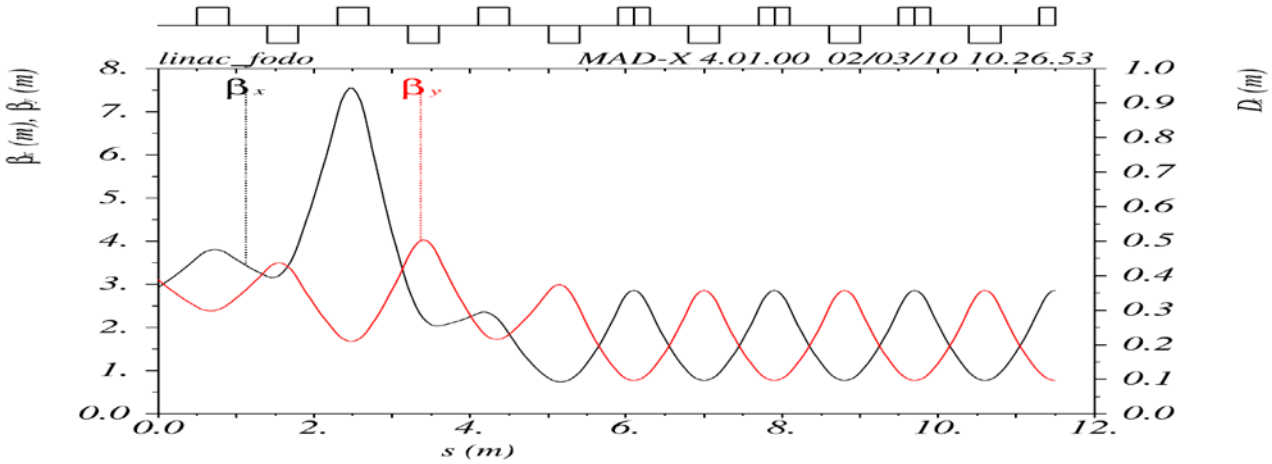

Figure 11 – Twiss functions in the matching system and first 3 FODO cells of the Injector Linac.

Table 13 – Parameters of the matching system.

Element	Length (cm)	Gradient (T/m)	Aperture radius (cm)
Q 16	40	0.7383	5
Q 17	40	-1.4163	5
Q 18	40	2.0155	5
Q 19	40	-1.9311	5
Q 20	40	1.7472	5
Q 21	40	-2.2061	5
L 22	64	-	5
L 23	50	-	5
L 24	50	-	5
L 25	50	-	5
L 26	50	-	5
L 27	50	-	5
L 28	50	-	5

Table 14 – Parameters of the FODO cells.

Element	Length (cm)	Strength K (m^{-2})	Aperture radius (cm)
Qd1	40	-4	5(20)
Qf1	40	4	5(20)
Lf1	50	-	5(3)

The strength of the quadrupoles in the FODO section is given by the coefficient K, with K = eG/P, where e is the charge of the e^-, G is the gradient and P is the longitudinal momentum of the particles. In order to have periodicity of the Twiss functions in every FODO cell, it is necessary to keep K constant for every cell. Since the longitudinal momentum of the particles increases along the linac, the gradient of the quadrupoles needs to increase proportionally. In the simulations it is assumed a linear increase of the momentum along the structures and zero increase between them. In Table 14 it is presented the aperture radius of the quadrupoles equal to 5 cm when they wrap the beam pipe and 20 cm (in parenthesis) when they wrap the structures. The aperture of the vacuum chamber is 5 cm between the structures, while the aperture radius of the structures is 3 cm (in parenthesis).

In the present design the strength of the quadrupoles in the FODO section is set to $K=\pm 4m^{-2}$. This means that at the start of the FODO section, when the beam energy is about 220MeV, the gradient in the quadrupoles is G=2.9 T/m. At the end of the section (after the 11^{th} structure) the beam energy is about 820MeV with the gradient of the quadrupoles set to 11.2 T/m. For a quadrupole wrapping an accelerating structure (with approximately 20 cm of radius aperture) that means magnetic field at the pole tip of 2.24T, which is too high because of iron saturation. One possibility to overcome this issue is lengthening the quadrupoles in the FODO section and/or reducing the final beam energy of the section. It will not be discussed in this paper.

3.5.2 Second section of Injector Linac

After the FODO section the focusing in the Injector Linac is provided by triplets of quadrupoles inserted between the accelerating structures (see Figure 12).

The first section of triplets is composed of 15 accelerating structures of the same type used in the FODO section, separated one from the other one by 4.3m of drift space.

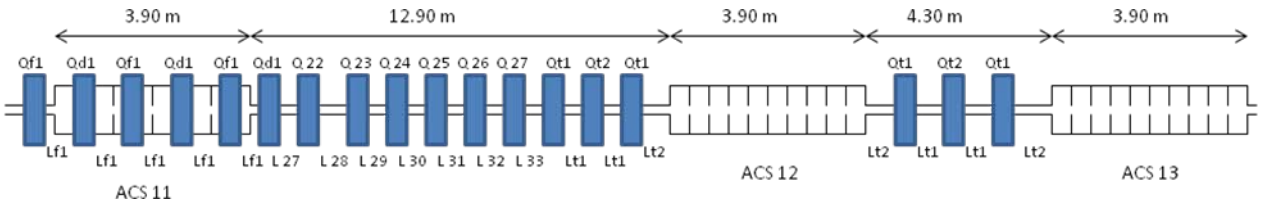

Figure 12 - Layout of the first section of triplets and its matching system.

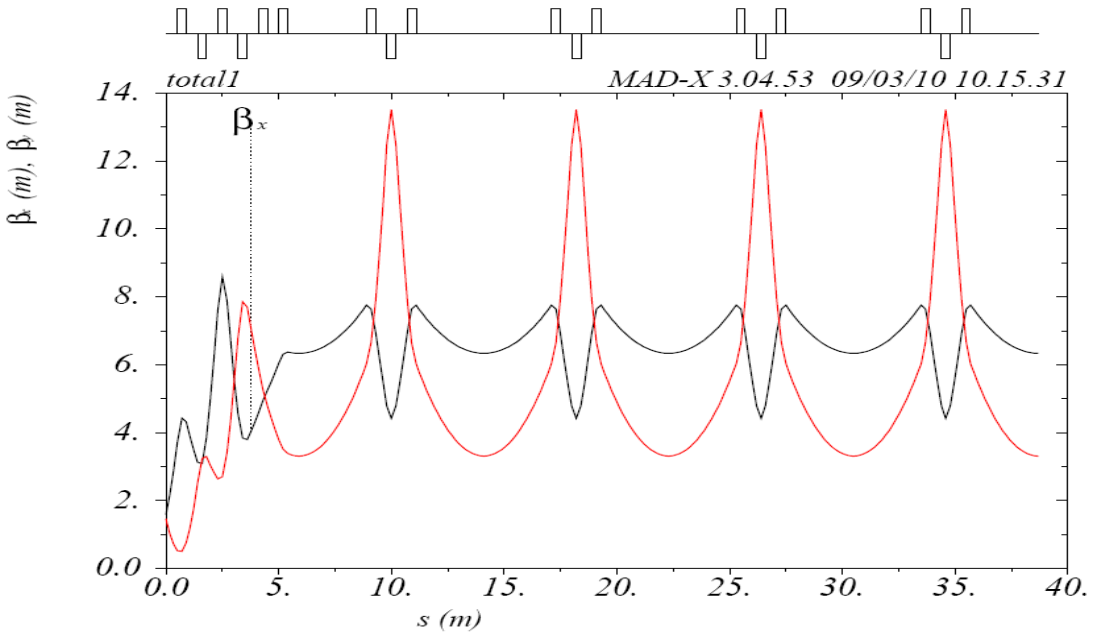

Figure 13 – Twiss functions for the first 4 triplets of the section and its matching quadrupoles.

After the 11th structure of the Injector Linac it is placed the quadrupole 'Qd1' of the 66th FODO cell followed by 6 quadrupoles (Q22-27) forming the matching optics of the first triplets section. After the matching quadrupoles and before the 12th structure it is placed the first triplet. In Table 15 the parameters of quadrupoles Q22-27 are reported, while in Figure 13 it is illustrated the optics up to the first 4 triplets of the section. Table 16 gives the parameters of the triplets.

Table 15 – Parameters of the matching system for the first triplets section.

Element	Length (cm)	Gradient (T/m)	Aperture (cm)
Q 22	40	7.1591	5
Q 23	40	-8.2265	5
Q 24	40	7.3451	5
Q 25	40	-5.8143	5
Q 26	40	0.4322	5
Q 27	40	1.1685	5
L 28	75	-	5
L 29	50	-	5
L 30	50	-	5
L 31	50	-	5
L 32	50	-	5
L 33	50	-	5
L 34	350	-	5

Table 16 – Parameters of the triplets in the first triplets section.

Element	Length (cm)	Strength K (m^{-2})	Aperture (cm)
Qt1	40	1	5
Qt2	40	-2	5
Lt1	50	-	5
Lt2	105	-	5

In this section (like in the preceding one) the gradient of the quadrupoles in the triplets has to increase proportionally to the longitudinal momentum. The gradient of the first 'Qt1' quadrupoles is G=2.8T/m, the gradient of the first 'Qt2' is G=-5.6T/m. At the end of the section the mean energy of the beam is 1.66GeV, and the gradient of the 15th triplet is G=5.4T/m for 'Qt1' and G=10.9T/m for 'Qt2'.

3.5.3 Third section of Injector Linac

In order to prevent the gradient of the quadrupoles from becoming too high, at this point a second triplets section is designed to accelerate the beam up to the PDR injection energy. This section is composed of 21 accelerating structures spaced by 4.3m of drift like in the previous section. Its optics is also similar, with the focusing of the beam provided by triplets inserted between the structures. As it is showed in Figure 14, after the 26th structure of the Injector Linac it is placed a system of 6 quadrupoles (Q 28-33) used to match the beam to the new optics, followed by the first triplet of the second triplets section 'Qt3'-'Qt4'-'Qt3' and the first accelerating structure of the section. The optics of matching quadrupoles and first 4 triplets of this section is presented in Figure 15.

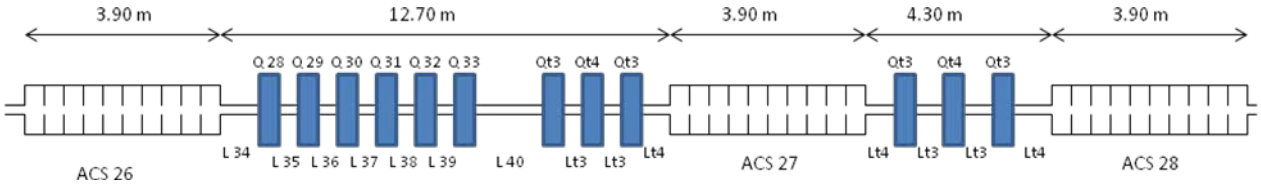

Figure 14 – Layout of the second triplet section and its matching system.

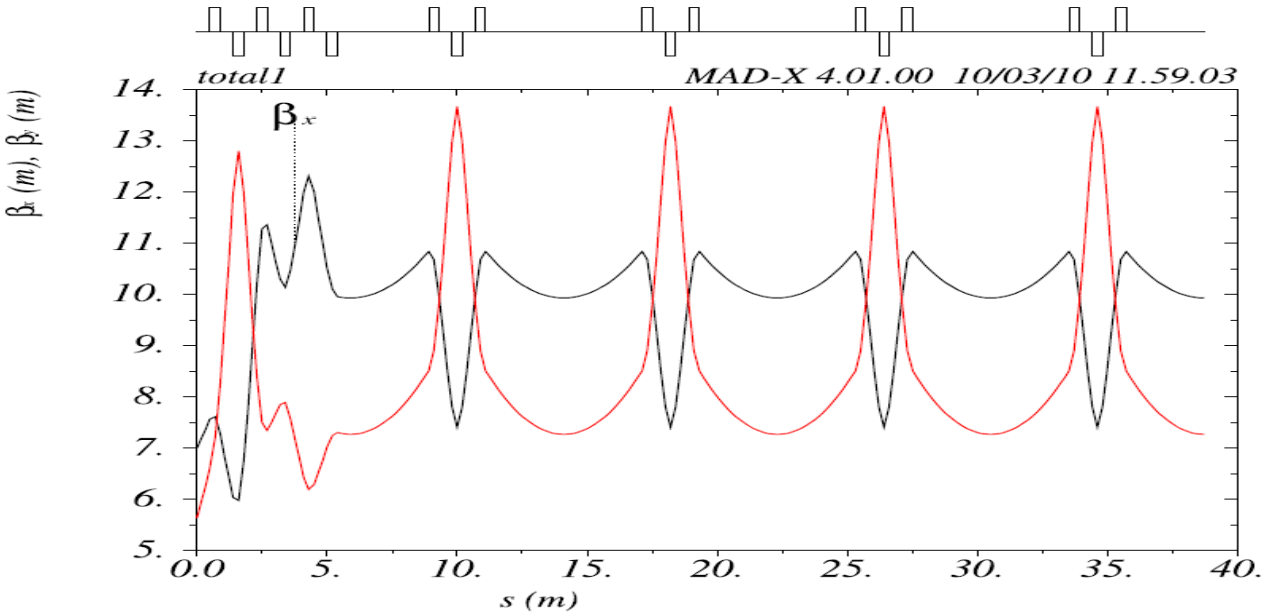

Figure 15 - Optics of the second triplet section (first 4 triplets) and its matching system.

In Table 17 the parameters of the matching system are reported, while in Table 18 the parameters of the triplets are presented.

Table 17 – Parameters of the matching system in Figure 14.

Element	Length (cm)	Gradient (T/m)	Aperture (cm)
Q 28	40	3.724	5
Q 29	40	-9.1164	5
Q 30	40	6.4467	5
Q 31	40	-3.2672	5
Q 32	40	3.6483	5
Q 33	40	-1.7676	5
L 34	105	-	5
L 35	50	-	5
L 36	50	-	5
L 37	50	-	5
L 38	50	-	5
L 39	50	-	5
L 40	350	-	5

Table 18 – Parameters of the triplets in the second triplets section.

Element	Length (cm)	Strength K (m^{-2})	Aperture (cm)
Qt3	40	0.65	5
Qt4	40	-1.3	5
Lt3	50	-	5
Lt4	105	-	5

For the first triplet the gradient is 3.6T/m and -7.2T/m, while for the 21st triplet the energy of the beam is 2.78 GeV and the gradients are 6.1T/m and -12.1T/m.

General parameters of the Injector Linac are presented in Table 19.

Table 19 – General parameters of the Injector Linac.

Parameter	Unit	Value
Total length	m	377.2
Average accelerating field	MV/m	14.6
Number of accelerating structures		47
Length of accelerating structures	m	3.9
Number of quadrupoles		192
Quadrupoles length	m	0.4

4. Beam parameters at the end of the Injector Linac and Pre-Damping Ring acceptance

The beam parameters at the end of the Injector Linac are listed in Table 20. In Figures 16 and 17 are reported pictures of the phase space of the positron beam.

Table 20 – Beam parameters at the end of the Injector Linac.

Beam Parameter	Unit	Value
Mean energy	MeV	2825
Yield	e^+/e^-	0.70
Horizontal Normalized Emittance (rms)	mm mrad	7685
Vertical Normalized Emittance (rms)	mm mrad	8105
Energy spread (rms)	%	4.5
Bunch length (rms)	mm	5.4

The nominal beam energy is 2.86GeV; however a maximum number of e^+ inside the Pre-Damping Ring acceptance is reached for the beam mean energy reported in Table 20.

In order to have the required number of positrons at the interaction point and taking into account the transport efficiency, $4.6 \cdot 10^9$ positrons per bunch should be accepted in the PDR [3]. Therefore, it is important to check how many particles of the beam at the injection effectively lie inside the Pre-Damping Ring's acceptance. According to [13], the current design assumes transverse emittance of the beam equal to 7000 mm mrad, with a geometrical acceptance of 6 times the rms bunch size in both horizontal and vertical planes. Figure 16 shows that the beam fits pretty well in the transversal acceptance.

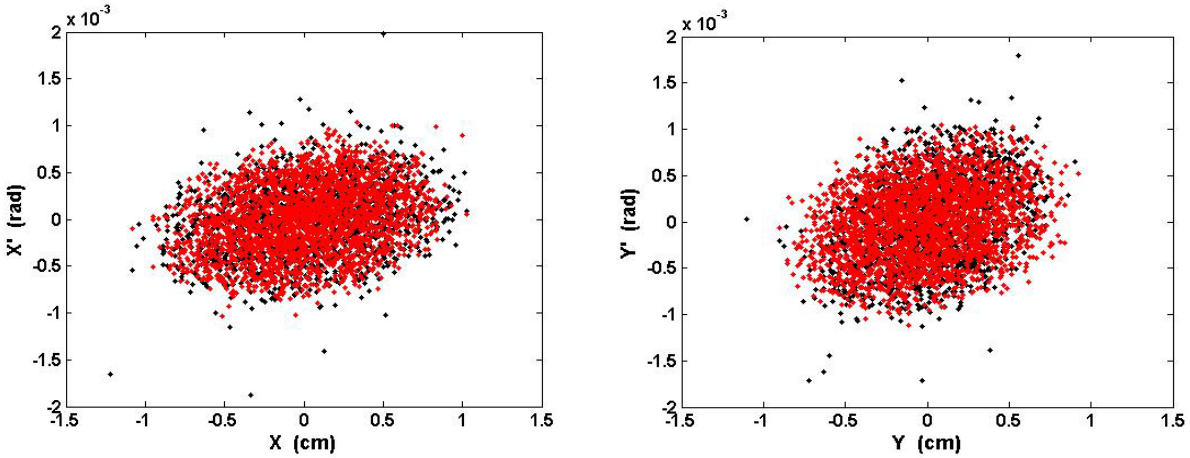

Figure 16 – Horizontal (left) and vertical (right) phase space of the positron beam at the end of the Injector Linac. Points in red lie inside the acceptance of the PDR (current design).

As an effect of the curvature of the RF field, the energy spread of the beam is pretty high and only part of the beam lies inside the energy acceptance (see Figure 17). In the current design of the PDR the reference energy is 2.86GeV with an energy acceptance of ±1.2%. However future design could increase this value [14].

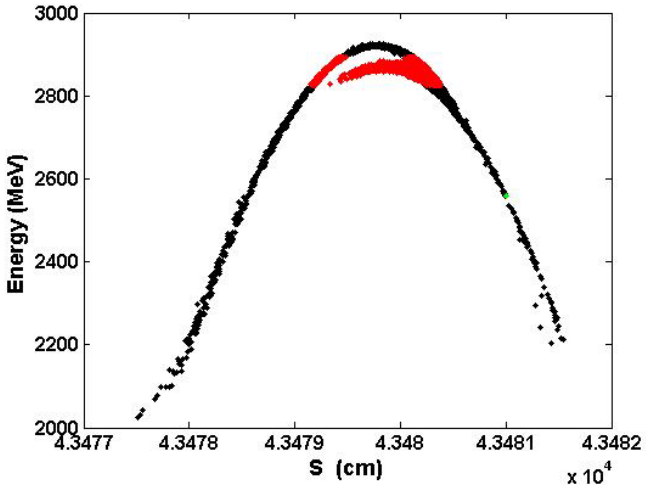

Figure 17 – Longitudinal phase space of the beam at the end of the Injector Linac. Points in red lie inside the energy acceptance of the PDR (current design).

Table 21 gives the final accepted yield of positrons in the PDR calculated for different energy acceptances. As it can be seen, an increase of the yield would be obtained by increasing the current value of 1.2%.

Table 21 – Positron yield for different values of the energy acceptance of the Pre-Damping Ring.

Energy Acceptance %	**Yield (e^+/e^-)**
1.2	0.453
2	0.561
3	0.619

Taking into account the yield corresponding to the current design of the PDR, a value of 1.63 nC for the bunch charge is required in the e^- beam impinging the crystal. Applying the results of [6], it would imply a PEDD equal to 30 J/g. A value of the PEDD lower than 35 J/g is considered safe for the target survivability.

For the 500GeV configuration, with double charge, the value of the PEDD is also doubled, exceeding then the safety value for the amorphous target survivability. Therefore for this configuration the construction of 2 target stations will be implemented, including crystal, bending magnet, amorphous target and solenoid/Pre-Injector Linac. The primary electron beam will be produced like for the 3TeV configuration (but with double charge per bunch) and accelerated by the 5GeV linac. At this point an RF deflector will split each train in 2 halves, sending half of the total number of bunches in each station. The positrons are then produced in parallel with no variation of the PEDD in each target station. Downstream the 2 Pre-Injector Linacs, another RF deflector will recombine the 2 halves of the trains, upstream the Injector Linac (at 200 MeV).

5. Conclusion

In this paper, a design of the CLIC non-polarized positron source is presented.

For the 3 TeV configuration, the baseline assumes a single station with hybrid targets using channeling. The capture and acceleration of e^+ have been optimized and the beam transported up to the end of the Injector Linac at 2.86GeV. The present simulations show that the required number of e^+ is achieved and delivered to the Pre-Damping Ring without feasibility issues.

For the 500 GeV configuration, the CLIC positron source is based on two stations with hybrid targets using channeling and working in parallel. In this way it is possible to ensure target survivability without feasibility issues. Then when the charge will be reduced, for the 3 TeV configuration, one station will be used as spare one.

Future studies will be performed on:

- RF structures in the Pre-Injector Linac in order to increase the accelerating gradient.
- Injector Linac optics in order to relax the maximum gradient on some quadrupoles.
- Beam stability related to misalignments and wake field effects.

References

[1] F. Tecker et al., "2008 CLIC Parameters List", CLIC-Note 764, available at http://clic-study.web.cern.ch/CLIC-Study/Design.htm .

[2] "CLIC Main Parameters evolution from 500GeV to 3TeV", available at http://clic-study.web.cern.ch/CLIC-Study/Design.htm .

[3] L. Rinolfi, "CLIC Main Beam Injector Complex review", CLIC09 Workshop, CERN, 12-16 Oct 2009, available at http://indico.cern.ch/ .

[4] R. Chehab et al., "Study of a positron source generated by photons from ultra-relativistic channeled particles", PAC 1989, Chicago, March 1989.

[5] R. Chehab et al., "An Hybrid Positron Source using Channeling for ILC", International Linear Collider Workshop 2010 LCWS10 and ILC10, Beijing, March 26-30 2010, available at http://lcws10.ihep.ac.cn/ .

[6] O. Dadoun et al., "Study of a hybrid positron sources using channeling for CLIC", CLIC-Note 808, 2010.

[7] R. Chehab, "Positron Sources", in CAS report CERN 94-01, Vol. II.

[8] K. Flöttmann, "Astra - A Space Charge Tracking Algorithm", available at http://www.desy.de/~mpyflo/ .

[9] Poisson Superfish code, available at http://laacg.lanl.gov/laacg/services/ .

[10] A. Ferrari, A. Latina, L. Rinolfi, "Design Study of the CLIC Injector and Booster Linacs with the 2007 Beam Parameters", CLIC-Note 737, 2008.

[11] MAD-X, http://mad.web.cern.ch/mad/ .

[12] CSRtrack, http://www.desy.de/xfel-beam/csrtrack/ .

[13] F. Antoniou, "CLIC Pre-Damping Rings overview", CLIC09 Workshop, CERN, 12-16 Oct 2009, available at http://indico.cern.ch/ .

[14] F. Antoniou, private communication, CERN, 2010.